This is the peer reviewed author accepted manuscript (post print) version of a published work that appeared in final form in:

Joyce, Paul, Wignall, Anthony, Peressin, Karl, Wright, Leah, Williams, Desmond B, Prestidge, Clive A 2022 'Chitosan nanoparticles facilitate improved intestinal permeation and oral pharmacokinetics of the mast cell stabiliser cromoglycate', International Journal of Pharmaceutics, vol. 612, article no. 121382

This output may not exactly replicate the final published authoritative version for which the publisher owns copyright. It is not the copy of record. This output may be used for non-commercial purposes. This version is licensed under a Creative Commons CC-BY-NC-ND 4.0 license (http://creativecommons.org/licenses/by-nc-nd/4.0/).

The final definitive published version (version of record) is available at: https://doi.org/10.1016/j.ijpharm.2021.121382

Persistent link to the UniSA Research Outputs Repository: https://researchoutputs.unisa.edu.au/11541.2/28832

General Rights

Copyright and moral rights for the publications made accessible in the UniSA Research Outputs Repository are retained by the authors and/or other copyright owners and it is a condition of accessing publications that users recognize and abide by the legal requirements associated with these rights.

- Users may download and print one copy for the purpose of private study or research.
- You may not further distribute the material or use it for any profit-making activity or commercial gain
- You may freely distribute the persistent link identifying the publication in the UniSA Research Outputs Repository

If you believe that this document breaches copyright, please contact us and provide details. We will remove access to the work immediately and investigate your claim.

Chitosan Nanoparticles Facilitate Improved Intestinal Permeation and Oral Pharmacokinetics of the Mast Cell Stabiliser Cromoglycate

Paul Joyce,[a ‡] *Anthony Wignall,*[a ‡] *Karl Peressin,*[a] *Leah Wright,*[a] *Desmond B Williams,*[a] *and Clive A. Prestidge*[a]*

[a] UniSA Clinical & Health Sciences, University of South Australia, Adelaide, South Australia 5000, Australia

[‡] Equal contribution.

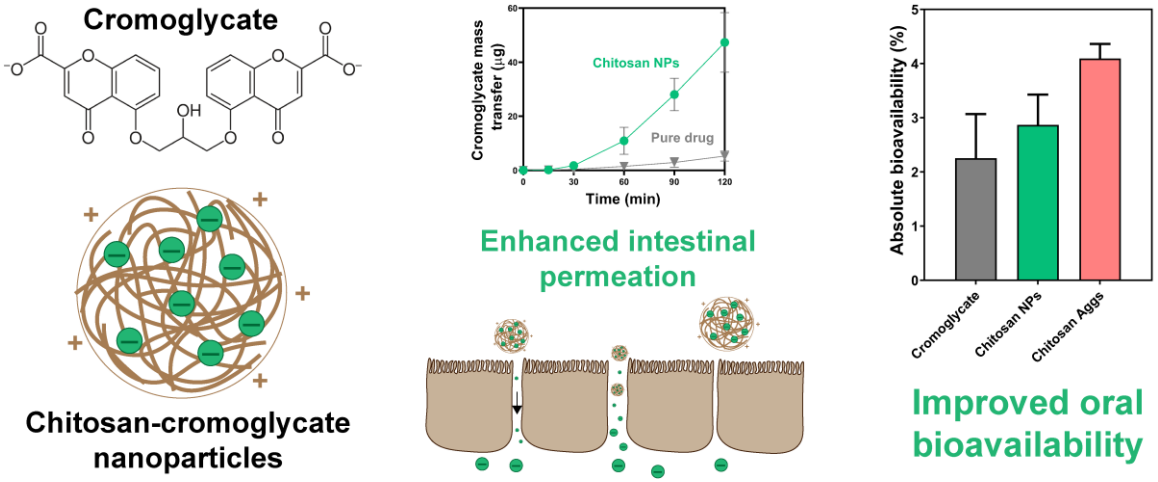
*Corresponding Author. Email: clive.prestidge@unisa.edu.au

Abstract

Cromoglycate is a mast cell stabiliser typically administered via inhalation or intranasally for the treatment of allergy-based respiratory issues. Oral dosing of cromoglycate remains challenging due to its high solubility but low permeability across epithelial membranes in the gastrointestinal tract: effective formulation strategies are clearly needed. Here, we investigate and preclinically develop chitosan-cromoglycate complexes and associated nano/microparticle formulations with muco-adhesive and permeation enhancing capabilities to overcome the biopharmaceutical challenges for oral dosing. The synthesized complexes were optimized with respect to chitosan grade, particle size, and drug loading and demonstrated up to a 9.3-fold enhancement in permeability across a Caco-2 monolayer for chitosan-cromoglycate particles, compared to the pure drug. This increased intestinal permeability led to improved pharmacokinetic performance of cromoglycate, e.g. up to 1.82-fold increase in relative oral bioavailability when dosed to Sprague-Dawley rats in a fasted state. These findings confirm the potential for chitosan particles to serve as an effective oral delivery vehicle for cromoglycate, with additional formulation optimization presenting the opportunity to reduce dosing frequency for treatment of allergy-based respiratory ailments.

Keywords: oral delivery, chitosan, cromoglycate, cromoglicic acid, intestinal permeation, poorly permeable drugs.

Graphical abstract



1. Introduction

Cromoglycate (cromoglicic acid) belongs to a class of drugs known as cromones which act to inhibit the release of inflammatory mediators from mast cells. The administered drug is typically the disodium salt of cromoglycate, which is a Biopharmaceutical Classification System (BSC) Class III drug with reported intestinal bioavailability of approximately 1% [1] and a biological half-life of 45 to 100 min [2]. Poor oral bioavailability and rapid clearance of cromoglycate from the body has resulted in nasal administration as the predominant regimen for clinical dosing, with a reported bioavailability of 7% [1, 3-5]. Treatments are generally administered as 5 mg doses via aerosol inhalation multiple times daily for the preventative treatment of allergy-based respiratory ailments [5]. The need for multiple treatments per day is often met with low patient compliance due to inconvenience, which introduces the propensity for sub-therapeutic levels of the bioactive within systemic circulation.

In light of this, there exists an urgent demand for improved cromoglycate formulations that improve patient compliance by enhancing bioavailability through an acceptable mode of administration to ultimately reduce the frequency of dosing required. Oral administration remains the most accepted delivery route for patients, resulting in high compliance to prescribed dosing programs [6, 7]. It is, however, a challenge to achieve therapeutically relevant blood drug concentrations following transport across gastrointestinal epithelia [8] for hydrophilic ionic molecules such as cromoglycate (M_r dianion 466.4 g.mol, pK_a <1.9), since the drug molecules cannot diffuse freely across epithelial cell membranes due to their high molecular weight, charge and hydrophilicity [9-11]. Paracellular transport is therefore required for systemic absorption from the small intestine [7, 12], however, this pathway is restricted by tight junctions [13, 14], which offer a smaller surface area for transport as compared to the transcellular pathway [15] and generally require manipulation to allow passage, resulting in

inadequate absorption and comparatively poor systemic availability of the administered drugs [16].

Irrespective of the transport pathway required, gastrointestinal epithelia are protected by thick layers of mucus, which pose another significant biological barrier for drug penetration [17-24]. Rapid secretion and clearing of the mucus can limit the effectiveness of delivery systems [25], as many types of particles are efficiently trapped and cleared, making controlled release in the gastrointestinal tract difficult [25-27]. In addition to the viscosity of mucus, a major component, mucin, has been found to limit penetration of particles based on both charge and size [28]. Subsequently, a delivery vehicle that can effectively promote paracellular transport as well as muco-adhesion and permeation is required to transport cromoglycate from the GI tract to the systemic bloodstream.

One proven formulation approach for increasing the oral bioavailability of poorly permeable hydrophilic drugs is through chitosan complexation, where the chitosan serves as a muco-adhesive permeation enhancer that increases the residence time of the drug at the site of absorption, while also regulating the transient opening of tight junctions to promote paracellular absorption [29]. The bio-enabling mechanisms of chitosan are driven by its polycationic nature at acidic pH, where its cationic surface charge electrostatically interacts with the negative charges of mucus and cell membranes [30-32]. Owing to these unique properties, chitosan has been widely exploited for drug delivery applications, where muco-adhesion and intestinal permeability of conjugated drugs can be modulated based on the molecular size, degree of acetylation and the counterion used to balance the cationic charge of chitosan [33-37].

The surface chemistry of chitosan lends itself as the ideal delivery vehicle for hydrophilic and poorly permeable anions, since chitosan-drug complexes readily form via electrostatic interactions. Subsequently, a wealth of studies have highlighted the capacity for chitosan to

improve the bioavailability of poorly permeable anionic drugs with similar chemistries to cromoglycate [33-35, 37-47]. Since cromoglycate has two anionic sites at biologically relevant pH, it can either be complexed with preformed cationic nanoparticles that are synthesized via the use of a crosslinker, such as tripolyphosphate (TPP), or it can be used as a crosslinking agent itself to form nanoparticles where its anionic sites serve as ionic bridges (and thus avoids the need for an additional crosslinking agent) [4]. Drug loading efficiency through these complexation methods is dependent on the number of cationic sites available, which is determined by the polymer size, degree of deacetylation and the pH of the solution.

Despite previous studies highlighting the capacity for cromoglycate to be successfully complexed with chitosan, such complexes have not been investigated for oral drug delivery. Instead, attention has remained on the ability for chitosan to facilitate muco-adhesion and permeation for intranasal administration. However, due to the well-established capacity for chitosan nanoparticles to improve oral delivery performance [48], we hypothesized that complexing cromoglycate with chitosan particles of optimal size can facilitate improved muco-adhesion and penetration within the intestine, thus prolonging drug exposure at the absorption site, while also promoting opening of the epithelial tight junctions to increase oral bioavailability. As such, the aim for this study was to synthesize chitosan particles using cromoglycate as a crosslinking agent, in combination with TPP, and investigate *in vitro* drug permeation across a model Caco-2 monolayer, as well as *in vivo* pharmacokinetics in Sprague-Dawley rats. By evaluating the performance of chitosan-cromoglycate complexes for oral delivery, the insights derived from this study will provide clear direction for the future optimisation of cromoglycate drug delivery vehicles with the aim of moving towards an effective, once-per-day oral dosing regimen to improve patient compliance.

2. Experimental Section

2.1. Materials

Sodium cromoglycate, pravastatin sodium, chitosan [low (50-190 kDa) and medium (190-310 kDa) molecular weight (MW); degree of acetylation 15-25%] and sodium triphosphate pentabasic were purchased from Sigma-Aldrich (Australia). Dulbecco's modified eagle medium (DMEM), Hanks balanced salt solution (HBSS), foetal bovine serum (FBS), penicillin-streptomycin and L-glutamine were purchased from Thermo Fisher Scientific (Life Technologies, Australia). FaSSIF/FeSSIF/FaSSGF powder was purchased from Biorelevant.com (London, UK). All other chemicals and solvents were of analytical grade or greater and used as received. High purity (Milli-Q) water was used throughout the study.

2.2. Synthesis of Chitosan-Cromoglycate Complexes

Chitosan-cromoglycate complexes were prepared by an ionic gelation method [36, 49]. Briefly, an aqueous sodium cromoglycate solution (5 mg/mL) was added dropwise to a chitosan solution (3 mg/mL) in 1% v/v acetic acid under vigorous stirring for 15 min. Complexes were prepared at a chitosan-to-cromoglycate ratio of 5:1 or 5:2 with both low and medium MW chitosan to optimise drug loading and particle size. Chitosan-cromoglycate aggregates (CC_{Aggs}) were formed through lyophilization of the synthesized precipitates for a minimum of 24 h to obtain a dry powder, which was resuspended immediately prior to use.

Chitosan-cromoglycate nanoparticles (CC_{NPs}) were synthesized by adding an aqueous solution of sodium tripolyphosphate (10 mg/mL) dropwise to the chitosan-cromoglcyate solution in acetic acid and homogenized for 10 min at 14 000 rpm. The resulting dispersion was sonicated for 1 h at ambient temperatures before being centrifuged for 20 min at 18 000 rpm to precipitate the particles and remove any unbound cromoglycate. Precipitated pellets were redispersed with aid of sonication immediately prior to use.

2.3. Characterization of Chitosan-Cromoglycate Complexes

2.3.1. Drug Loading & Encapsulation Efficiency

Cromoglycate loading within CC_{NPs} was calculated via the quantification of unbound cromoglycate following particle formation, according to a previous study [48]. That is, supernatants were collected and appropriately diluted with mobile phase prior to quantification via High Performance Liquid Chromotograph (HPLC). Samples were eluted through an Alltech LiChrospher RP C18 analytical column (5 µm x 4.6 mm ID x 250 mm) maintained at 40 °C by HPLC (Shimadzu, Japan). Isocratic elusion flow rate 1.0 mL/min, mobile phase acetonitrile: 20 mM potassium dihydrogen orthophosphate (25:75), UV detector 240 nm, injection volume 30 µL, cromoglycate retention time of approximately 2.25 min. Drug loading was not calculated for CC_{Aggs} as the entire formulation was lyophilised and dosed as a resuspension of the powder, and thus it was assumed that the encapsulation efficiency of CC_{Aggs} was 100%.

2.3.2. *Particle Sizing & Zeta Potential*

The hydrodynamic size of CC_{NPs} samples was determined using dynamic light scattering (Zetasizer Nano ZS, Malvern, UK). Each sample was dispersed at an equivalent concentration in Milli-Q water (refractive index = 1.33) prior to analysis. Particle sizes of the CC_{Aggs} samples were characterized using laser diffraction (Mastersizer 2000, Malvern, UK) over a period of 5 min in water (refractive index = 1.33). Stirrer and pump speeds were set to 500 and 1250 rpm, respectively. The size analysis results are expressed as the volume (v) diameter at 90% cumulative volume, designated as D (v,0.9). Zeta potential measurements were completed using a Zetasizer Nano ZS for pure cromoglycate, pure chitosan, CC_{NPs} and CC_{Aggs} dispersed in a 0.9% NaCl solution.

2.3.3. *Particle Morphology*

The surface morphologies of low molecular weight chitosan nanoparticles were examined using scanning electron microscopy (SEM) (Zeiss Merlin, Oberkochen, Germany) and transmission electron microscopy (TEM) (JEOL JEM-1200 EX II, Tokyo, Japan). For SEM,

samples were applied to double-faced adhesive carbon tape and coated with 10 nm platinum preceding imaging at an accelerating voltage of 1 kV. For TEM, nanoparticles were suspended in ethanol at a concentration of 1 mg/mL via sonication for 1 h. Samples (5 µL) were transferred to copper grids and left to air dry for > 30 min to allow for complete ethanol evaporation. TEM analysis was performed at an accelerating voltage of 120 kV.

2.4.In Vitro Cromoglycate Release Study

Cromoglycate release studies from CC_{NPs} and CC_{Aggs} were performed using a two-step gastrointestinal model to simulate exposure to gastric and intestinal media with biologically relevant concentrations of bile salts and phospholipids. Briefly, fasted state simulated gastric fluid (FaSSGF; pH 1.6) was prepared by dissolving 2.00 g NaCl in 1 L Milli Q water and adjusting the pH with 0.2 M HCl, prior to the addition of 0.06 g FaSSIF/FeSSIF/FaSSGF biorelevant powder. Fasted state simulated intestinal fluid (FaSSIF) was prepared by dissolving 2.24 g FaSSIF/FeSSIF/FaSSGF powder in 1L pH 6.5 buffer (0.42 g NaOH, 3.4 g NaH_2PO_4, 6.2 g NaCl, 1L MilliQ). Cromoglycate release kinetics were observed for 90 min; a 30 min gastric step followed by a 60 min intestinal step. The experimental procedure was initiated with the addition of cromoglycate complex, equivalent to 3 mg cromoglycate, into a temperature-controlled reaction vessel containing 10 mL of freshly prepared FaSSGF (37 °C, pH 1.6). After 31 min, 20 mL of FaSSIF media was added (pH 6.5) to the reaction vessel and the pH was automatically adjusted by a pH-stat apparatus (Metrohm 902 Titrando, Herisau, Switzerland) to maintain pH at 6.5 ± 0.01. Aliquots (100 µL) were taken periodically and centrifuged for 5 min at 22 000 rpm, where the supernatant was collected and analyzed using HPLC to quantify cromoglycate release. The final aliquot for the gastric phase was taken at 30 min, prior to additional of FaSSIF media. Since the total volume of aliquots withdrawn from the release buffer during sampling represented only 2.3% of the total buffer solution (*i.e.* 700 µL was

withdrawn from 30 mL over the 90 min period), it was assumed that the amount of drug withdrawn from solution was negligible and as a result, this was not analyzed.

2.5.In Vitro Cromoglycate Permeation Study

Caco-2 cells were cultured in DMEM supplemented with 10% FBS, 1% penicillin-streptomycin and 1% L-glutamine. Cell cultures were maintained at 37 °C, 95% relative humidity and 5% CO_2. Culture medium was changed every second day after being washed with PBS. Cells were seeded at a density of 2 x 10^5 cells/mL and cultivated for a minimum of 21 d to reach confluency and ensure monolayer differentiation. Growth media were replaced every 12 to 24 h to prevent cellular adaptation to a starved phenotype. The integrity of the Caco-2 monolayer was established by measuring transepithelial electrical resistance (TEER) across the monolayer using an EVOM2 (World Precision Instruments, Sarasota, FL). Prior to initiation of permeation studies, Caco-2 monolayers were washed with HBSS to remove non-adherent cells. Monolayers were then equilibrated with the transport media for 30 min at 37 °C. The experiment was initiated via the addition of 0.4 mL pre-warmed formulation dispersed in HBSS at a cromoglycate equivalent dosage of 1 mg/mL to the apical chamber and 2.8 mL prewarmed HBSS into the basolateral chamber. At predetermined time intervals, 0.2 mL transport buffer was removed from the basal chamber and immediately replaced with 0.2 mL fresh prewarmed HBSS. Collected aliquots were appropriately diluted with HPLC mobile phase prior to HPLC analysis as described previously. All experiments were performed in triplicate and data are presented as the mean ± standard error. Apparent permeability coefficients (P_{app}) were calculated using Equation 1 below:

$$P_{app} = \frac{dQ}{dt} \times \frac{1}{A \times C_0} \qquad \text{Equation 1}$$

Where, dQ/dt is the steady-state flux, A represents the monolayer surface area, and C_0 represents the initial drug concentration in the apical chamber. TEER was measured at multiple time-points after dosing to establish the recovery of epithelial tight junctions.

2.6.In Vivo Pharmacokinetic Study

2.6.1. Dosing and Sample Collection

Pure cromoglycate and two optimized chitosan-cromoglycate complexes were selected for *in vivo* pharmacokinetic studies. Animal experiments were approved by the University of South Australia's Animal Ethics Committee (AEC project number U19-17). Male Sprague-Dawley rats (268 to 342 g) were divided into four groups (n = 3) and housed under controlled temperature, pressure and humidity levels. Animals were fasted overnight (12 to 15 h) with free access to water prior to the oral (PO) and intravenous (IV) administration. With exception of the IV dose of pure cromoglycate, which was suspended in saline solution (0.9% NaCl), all other formulations were suspended in Milli-Q water. All formulations were administered at equivalent cromoglycate dosage of 20 mg/kg. At predetermined time intervals up to 24 h post-dose, 0.2 mL blood samples were collected from the saphenous vein into pre-heparinised tubes. Plasma was separated immediately by centrifugation at 10 000 rpm for 5 min at room temperature and stored at -20 °C until extraction.

2.6.2. Extraction & Quantification of Cromoglycate Plasma Concentrations

Cromoglycate was extracted from rat plasma via solid phase extraction. 60 µL frozen plasma samples were thawed in the dark at room temperature prior to dilution with 170 µL of Milli-Q water. Sep-Pak C18 1cc cartridges (Waters, USA) were equilibrated with 1 mL methanol followed by 1 mL Milli-Q water. Diluted plasma samples were loaded onto the sorbent, then washed with 500 µL Milli-Q water to remove any residual impurities, before cromoglycate was eluted with 115 µL methanol. 5 µL of internal standard pravastatin sodium (75 µg/mL) was aliquoted into each sample and mixed by vortex mixing before liquid chromatography-mass spectrometry (LC-MS) analysis. Cromoglycate and pravastatin sodium was separated chromatographically using a Kinetex RP C18 analytical column (2.6 µm x 3 mm ID x 50 mm) maintained at a 40 °C by column oven (Shimadzu, Japan) under the following conditions:

isocratic flow rate 0.15 mL/min, injection volume 15 µL and run time 4.5 min. The API 3000 mass spectrophotometer (Sciex, USA) was operated in positive electrospray ionization for the ionization of both cromoglycate (m/z 496.0 > m/z 245.0) and internal standard (m/z 447.3 > m/z 142.9). The mobile phase was 42.5:42.5:15 methanol: acetonitrile: 2 mM ammonium acetate. The limit of detection and limit of quantification were found to be 2 ng/mL and 5 ng/mL, respectively.

Pharmacokinetic parameters for cromoglycate were obtained using GraphPad Prism software (Version 7.03). The area under the curve ($AUC_{0\text{-}inf}$) was calculated using the trapezoid rule, whereas maximum plasma concentration (C_{max}) and the time required to reach the maximum plasma concentration (T_{max}), were obtained directly from the individual plasma cromoglycate concentration versus time curves. The half-life of elimination ($T_{1/2}$) was calculated from the terminal slope of the elimination phase obtained from semi-logarithmic plots of the plasma cromoglycate concentration versus time.

3. Results and Discussion

3.1. Synthesis & Characterization of Chitosan-Cromoglycate Complexes

Chitosan-cromoglycate complexes were synthesized with varying chitosan molecular weights, dosing ratios and fabrication strategies to investigate the optimal conditions for maximising drug loading and encapsulation efficiency. For chitosan-cromoglycate nanoparticles (CC_{NPs}), fabrication with low molecular weight (LMW) chitosan at a chitosan-to-cromoglycate ratio of 5:1 led to the most efficient drug loading (10.3 ± 0.4%), demonstrated by an encapsulation efficiency of 83.1 ± 1.4% (Table 1). The average particle size of CC_{NPs}-LMW 5:1 was 174 ± 1.9 nm, with a polydispersity index of 0.21 (Supporting Information Figure S1), suggesting the particles were of a mostly monodisperse nature. This was supported by scanning and transmission electron micrographs which highlighted the spherical surface morphology and monodispersed nature of low molecular weight chitosan nanoparticles (Figure

1). Increasing the molecular weight of chitosan to medium molecular weight (MMW), reduced the encapsulation efficiency to 75.2 ± 1.6%, while also increasing the average particle size and decreasing the zeta potential of the complexes. The decrease in zeta potential, which inversely correlates with an increase in drug loading between complexes of the same chitosan molecular weight, can be explained by the decline in free surface cationic amine groups on chitosan particles due to enhanced ionic interactions with the anionic functional groups of cromoglycate.

Table 1: Drug loading and physicochemical characterization of fabricated chitosan-cromoglycate complexes.

Formulation[a]	Cromoglycate loading (%)	Encapsulation efficiency (%)	Particle size (PDI)[c]	Zeta potential (mV)
CC_{NPs}-LMW 5:1	10.3 ± 0.4	83.1 ± 1.4	174 ± 1.9 nm (0.21)	+ 23.0 ± 0.4
CC_{NPs}-LMW 5:2	17.5 ± 0.2	78.5 ± 1.0	7.21 ± 2.4 µm (0.73)	+ 19.0 ± 0.5
CC_{NPs}-MMW 5:1	9.40 ± 0.2	75.2 ± 1.6	234 ± 4.9 nm (0.18)	+ 19.6 ± 0.8
CC_{NPs}-MMW 5:2	15.4 ± 0.5	68.9 ± 2.1	5.51 ± 0.6 µm (0.61)	+ 16.4 ± 0.3
CC_{Aggs}-LMW 5:1	20.0	100[b]	129 ± 11 µm	+ 24.2 ± 2.9

CC_{Aggs}- LMW 5:2	40.0	100[b]	118 ± 26 µm	+ 21.8 ± 0.7

[a] Nomenclature of formulations: CC_{NPs} (chitosan-cromoglycate nanoparticles); CC_{Aggs} (chitosan-cromoglycate aggregates); LMW (low molecular weight chitosan); MMW (medium molecular weight chitosan); 5:1 (chitosan to cromoglycate ratio of 5:1); 5:2 (chitosan to cromoglycate ratio of 5:2).

[b] The encapsulation efficiency of CC_{Aggs} was 100%, since no drug was lost during the freeze drying process. However, it must be stated that this does not necessary represent a true encapsulation efficiency since some of the drug may be present as free drug and unbound to the chitosan particles.

[c] Particle sizing of CC_{Aggs} and CC_{NPs} was performed through laser diffraction and dynamic light scattering, respectively, using a refractive index of 1.33. CC_{Aggs} data is presented as *D* (v,0.9); CC_{NPs} data is presented as Z-average.

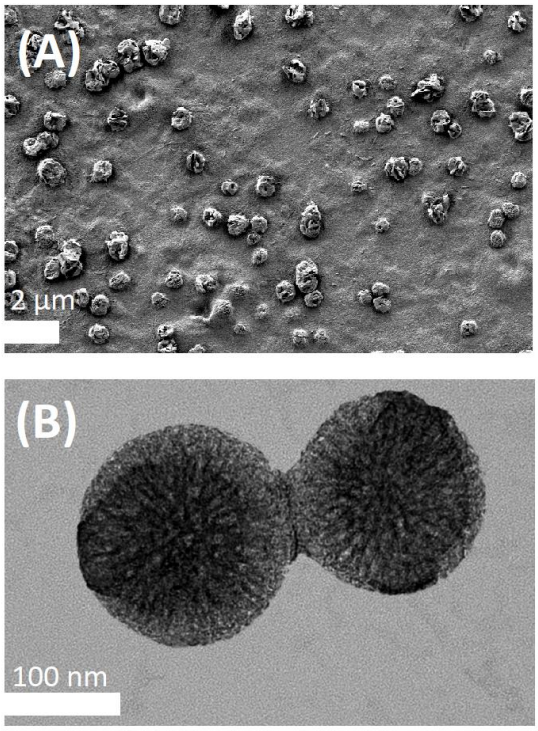


Figure 1: (A) Scanning and (B) transmission electron micrographs of low molecular weight chitosan nanoparticles.

While cromoglycate loading was enhanced at chitosan-to-cromoglycate ratios of 5:2, irrespective of the chitosan molecular weight employed, this strategy led to a reduction in encapsulation efficiency and more importantly, a drastic increase in particle size (*i.e.* > 5 µm). In doing so, this suggests that utilization of this concentration is suboptimal for the formation of CC_{NPs}, since it is hypothesized that the excess cromoglycate interferes with the crosslinking

mechanism required for nanoparticle synthesis. As such, only complexes prepared with a chitosan-to-cromoglycate ratio of 5:1 were pursued further with respect to analyzing *in vitro* permeation and *in vivo* bioavailability. Thus, the chitosan-to-cromoglycate ratio is no longer included within each abbreviation hereafter.

Fabrication of chitosan-cromoglycate aggregates (CC_{Aggs}), through the process of lyophilization, led to greater drug loadings (*i.e.* 20-40%) when compared to CC_{NPs}. However, this relies on the assumption that 100% of the cromoglycate is complexed with chitosan during the water removal process. Therefore, this hypothetical drug loading refers to both bound and unbound drug for CC_{Aggs}, whereas for CC_{NPs}, only bound drug remains within the complex. Particle size analysis of CC_{Aggs} via laser diffraction revealed diameters, *D* (v,0.9), between 118-148 μm, with no clear correlations existing between particle size and the chitosan grade or chitosan-to-cromoglycate ratio.

3.2.In Vitro Cromoglycate Release Kinetics

Cromoglycate release from chitosan complexes was investigated *in vitro* using a two-step gastrointestinal method that exposes each complex to media simulating the gastric (pH 1.6) and intestinal phase (pH 6.5). The intraluminal pH transitions from the highly acidic environment of the stomach to pH ≈ 6.0 in the duodenum and continues to gradually increase to pH ≈ 7.4 in the terminal ileum [50]; as such, drug formulations are exposed to an array of pH environments. Since chitosan has a pK_a of 6.5, a two-step *in vitro* model was selected to expose the chitosan-cromoglycate complexes to simulated gastric fluid, where the chitosan particles were expected to have a cationic charge, and to fluid simulating the proximal section of the small intestine, where the chitosan particles were expected to be neutral or mostly anionic. Cromoglycate release kinetics from each chitosan complex revealed multi-phase kinetics, where transition from the gastric phase to the intestinal phase triggered a rapid increase in drug release (Figure 2). This was attributed to a reduction in the cationic charge on

the chitosan surface, which limited the capacity for electrostatic complexation with cromoglycate, leading to pH-dependent drug release. It is expected that as the pH continues to increase above pH 6.5 during intraluminal transit, that the rate of cromoglycate release will also continue to increase.

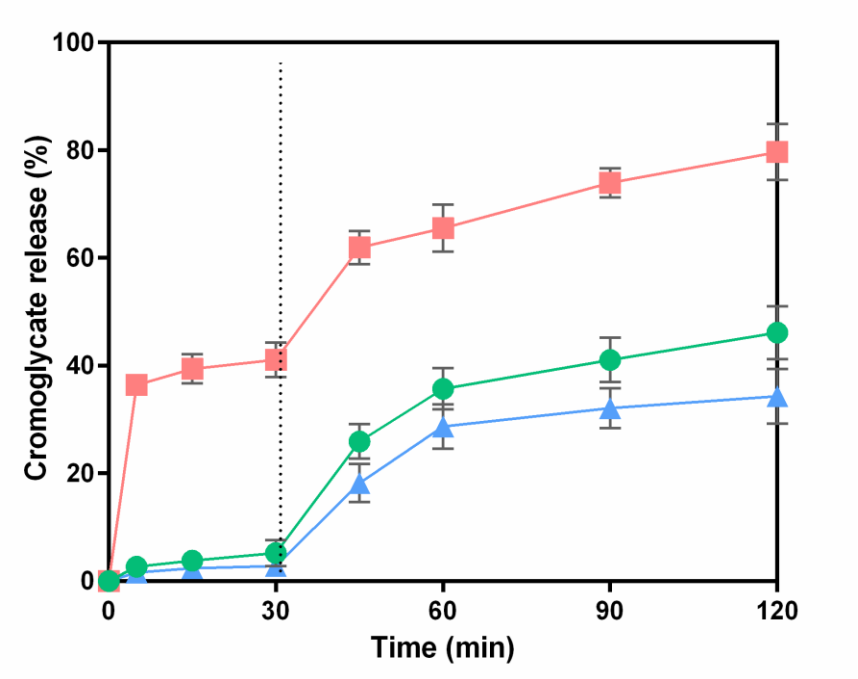


Figure 2: *In vitro* cromoglycate release in simulated gastrointestinal media for CC_{NPs}-LMW (green circles), CC_{NPs}-MMW (blue upward triangles) and CC_{Aggs}-LMW (red squares). The dotted line at 31 min separates the gastric phase from intestinal phase. Data represent mean ± SD (n = 3).

During the gastric phase, cromoglycate release was greatest from CC_{Aggs}-LMW, with 41.1 ± 3.2% of the initial dose being released within 30 min (Figure 2). This rapid drug release, especially when compared to both CC_{NPs} of varying molecular weight, is likely due to the higher degree of unbound cromoglycate within the complex. Since CC_{Aggs}-LMW were prepared via lyophilization, it was assumed that 100% of the drug was bound to the chitosan after the water removal step. However, this was unlikely to be the case and some drug was expected to remain within the powder as free drug. The drug release kinetics support this, where

36.4 ± 1.1% of the drug was released within the first 5 min, which is predicted to roughly correlate to the amount of free drug within the formulation.

In contrast to CC_{Aggs}-LMW, only a marginal degree of cromoglycate release (*i.e.* < 7%) was observed for CC_{NPs}-LMW and CC_{NPs}-MMW within the gastric phase. Instead, pH-triggered drug release was observed upon the transition towards intestinal media. This suggests that the majority of cromoglycate within the nanoparticle complexes existed as electrostatically bound drug, rather than free drug. Differences in the release kinetics between the two nanoparticle complexes suggested that increasing molecular weight delayed chitosan release, which is likely due to slight differences in chitosan pK_a and a slower rate of particle degradation. Importantly, these findings suggest that the nanoparticle synthesis approach may be most suitable for complexing cromoglycate, when compared to the aggregation approach, as it is critical that the drug remains bound to the carrier to ensure chitosan can facilitate muco-adhesion and intestinal permeation for improved oral bioavailability. Cromoglycate release from CC_{NPs}-LMW and CC_{NPs}-MMW was 46.1 ± 4.4% and 34.3 ± 5.1% after 90 min, respectively, which suggests a major portion of the cromoglycate will remain complexed to chitosan during intraluminal transit towards the terminal ileum. By doing so, this should maximise the potential for chitosan-facilitated permeation and absorption across the intestinal epithelium.

3.3. In Vitro Cromoglycate Permeation Study

In vitro intestinal permeation studies using Caco-2 monolayers were utilized to quantify the mass transfer of cromoglycate, when complexed with chitosan, across an epithelial cell monolayer. Caco-2 cells have been widely accepted as a model system for intestinal epithelial permeability [51] and tight junctions are known to be expressed between Caco-2 cells post-confluence [52-54]. Figures 3 displays the cromoglycate mass transfer and corresponding P_{app} for pure cromoglycate, CC_{NPs}-LMW, CC_{Aggs}-LMW and CC_{NPs}-MMW over a 120 min period. Pure cromoglycate exhibited the poorest permeability with only 0.6% of the initial dose

reaching the basolateral chamber, corresponding to a P_{app} of 0.66 x 10^{-6} cm/s; thus, confirming the impermeable nature of unformulated cromoglycate. The permeability of cromoglycate was increased substantially following the complexation with chitosan, as evidenced by 3.8 – 9.3-fold enhancements in P_{app}, thus demonstrating the capacity for chitosan to facilitate transport across the intestinal epithelial monolayer.

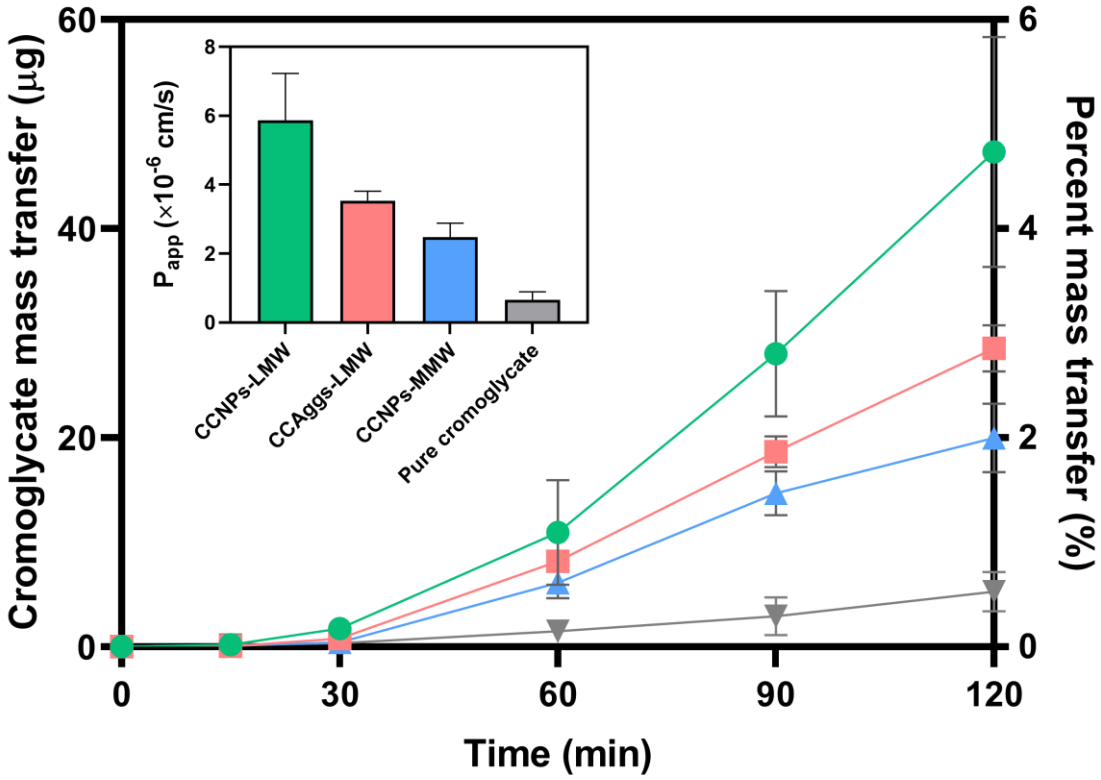


Figure 3: Total cromoglycate mass transfer (left y-axis) and percent mass transfer (right y-axis) across a Caco-2 monolayer for CC_{NPs}-LMW (green circles), CC_{Aggs}-LMW (red squares), CC_{NPs}-MMW (blue upward triangles), and pure cromoglycate (grey downward triangles). Inset: apparent permeability coefficients (P_{app}) corresponding to cromoglycate mass transfer for each formulation at an initial dose of 1 mg/mL. Data represents mean ± SD (n = 3).

Cromoglycate permeability across the Caco-2 monolayer was greatest for CC_{NPs}-LMW, with 47.3 ± 11 µg permeating across into the basolateral chamber. Since paracellular transport of

particles larger than 20 nm is not feasible in the absence of a permeation enhancer, due to a maximal widening of the intercellular space of ~15 nm [91, 92], it was predicted that CC_{NPs} induce the opening of tight junctions to allow the drug passage to the basolateral chamber. The increase in drug permeation for CC_{NPs}-LMW compared to CC_{Aggs}-LMW can be attributed to the smaller pore size, facilitating enhanced opening of tight junctions, and a reduction in the extent of premature cromoglycate release in biologically relevant media. However, CC_{Aggs}-LMW facilitated 1.43-fold greater permeation compared to CC_{NPs}-MMW, despite being ~50 times larger, which suggests that particle size was not the only driving force for facilitating transport.

Despite sharing similar physicochemical properties (*i.e.* particle size, zeta potential and drug loading) and *in vitro* drug release profiles, the degree of cromoglycate permeation between CC_{NPs}-LMW and CC_{NPs}-MMW was drastically different, suggesting facilitated drug transport was mediated in some part by chitosan molecular weight. The exact mechanism for this finding is not clear. However, previous studies have indicated that variations in paracellular transport, facilitated by chitosan nanoparticles, can be driven by chitosan molecular weight [55-57]. Schipper et al. [55] demonstrated that enhanced paracellular transport of 14C-mannitol was dependent on both chitosan's molecular weight and degree of acetylation (DA). That is, chitosan particles with a low DA (between 1 and 15%) were able to promote paracellular transport at both low and high molecular weights, but for chitosan with DA between 35 and 49% enhanced transport of 14C-mannitol was only observed at high molecular weights. As such, the findings of the current study suggest that low molecular weight chitosan is optimal for facilitating cromoglycate transport across epithelial monolayers for the degree of acetylation used in this study (15 – 25%). Furthermore, Huang et al. [58] demonstrated that chitosan nanoparticle uptake into epithelial cells increased with increasing molecular weight. This increased particle uptake may reduce the capacity for chitosan nanoparticles to interact

with and open the tight junctions between adjacent cells, thus exerting a detrimental effect for promoting paracellular transport. These observations highlight the importance for additional studies to fully elucidate the structural features of chitosan nanoparticles that lead to maximum cromoglycate transport.

Importantly, the current data suggests that fabrication of chitosan particles with TPP does not impact particle permeation, since both CC_{NPs}-LMW and CC_{NPs}-MMW were fabricated with TPP, whereas CC_{Aggs}-LMW were synthesized in the absence of TPP. Instead, these findings suggest that the zeta potential and molecular weight of chitosan is more important for epithelial permeation. However, it must be noted that the *in vitro* cellular monolayer model exists in the absence of gastrointestinal mucus, which is known to limit particle penetration based on hydrodynamic radius [28]. The Caco-2 model also represents a barrier where the formulation is in direct contact with the monolayer for the entire study, thus limiting any effect of enhanced particle mobility or flexibility. Based on these assumptions, it is predicted that the limited particle size effect observed *in vitro* would not correlate with *in vivo* findings due to the additional bio-barriers that each formulation will encounter *in vivo*.

Transepithelial electrical resistance (TEER) was monitored after exposing the Caco-2 monolayers to the chitosan complexes to demonstrate the capacity for chitosan to induce openings within the epithelial tight junctions. Figure 4 highlights the reduction in TEER 2 h after dosing CC_{NPs}-LMW and CC_{Aggs}-LMW to the Caco-2 monolayer, thus demonstrating the opening of tight junctions. Importantly, TEER recovered 24 h post-dosing, indicating the recovery of tight junctions and the presence of an intact and confluent monolayer. The capacity for chitosan to facilitate the transient opening of epithelial tight junctions is attributed to the electrostatic interactions between chitosan cationic amino groups and the negatively charged cell membranes which have been shown previously to induce the redistribution of key tight junction proteins, such as claudin-4 [59]. Ultimately, this mechanism enhanced cromoglycate

penetration across the Caco-2 monolayer into the basolateral chamber of the transwell system, which was predicted to enhance oral bioavailability compared to the unformulated drug.

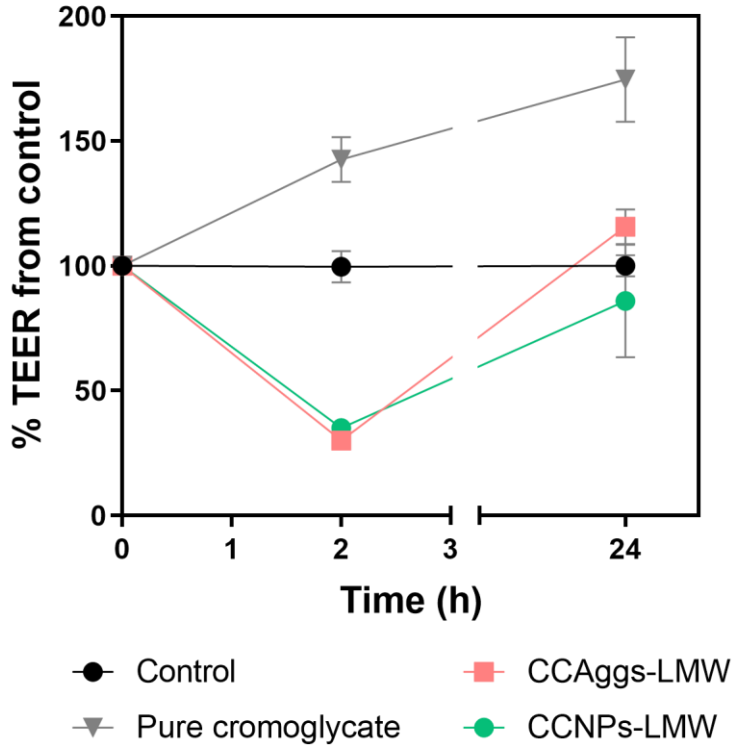


Figure 4: Time-dependent changes in TEER after exposure of Caco-2 monolayers to various cromoglycate formulations, in relation to an untreated monolayer (control group). Data represent mean ± SD (n = 3).

3.4.In Vivo Pharmacokinetics

CC_{NPs}-LMW and CC_{Aggs}-LMW were investigated for their ability to promote oral cromoglycate pharmacokinetics in Sprague-Dawley rats. CC_{NPs}-MMW was not investigated *in vivo* due to its poor capacity to enhance *in vitro* epithelial permeation of cromoglycate. The pharmacokinetic profile after a single dose of pure cromoglycate (20 mg/kg; no delivery excipients) via intravenous (IV) injection is presented in Figure 5, which highlights the rapid clearance of cromoglycate from the plasma through a two-phased plasma clearance, with the initial phase observing a half-life of 0.09 ± 0.01 h (5.4 min) owing to rapid distribution into

tissue (Table 2). This was followed by a slower secondary phase characterised by a half-life of 4.31 ± 0.6 h. In contrast, oral administration (PO) of pure cromoglycate revealed rapid absorption with a maximum plasma concentration of 29.6 ± 5.2 ng/mL at 0.81 ± 0.3 h. This was followed by a rapid decline in plasma cromoglycate concentrations below the limit of quantification after 10 h (Figure 6), characterised by a plasma half-life of 2.14 ± 0.6 h. Comparisons between the area-under-the-curve ($AUC_{0\text{-}inf}$) between oral and IV dosing revealed an absolute oral bioavailability (F_{ABS}) of 2.25 ± 0.7%.

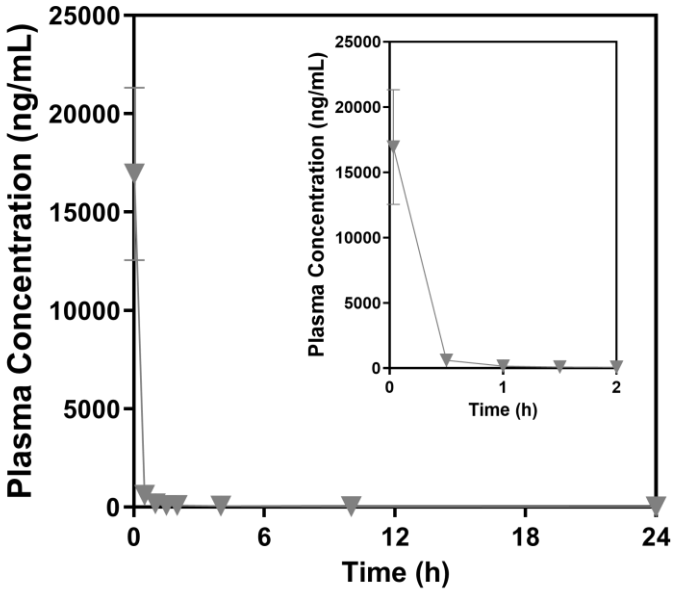


Figure 5: Plasma cromoglycate concentration time profile following intravenous administration (20 mg/kg) in Sprague Dawley rats. Data represent mean ± SD (n = 3).

Table 2: Pharmacokinetic parameters of cromoglycate following a single dose (20 mg/kg) for various dosage forms (*i.e.* IV or PO) and various chitosan-cromoglycate complexes in Sprague Dawley rats. Data represents mean ± SD (n = 3).

Parameter	**Pure cromoglycate (IV)**	**Pure cromoglycate (PO)**	**CC_{Aggs}-LMW (PO)**	**CC_{NPs}-LMW (PO)**

T_{max} (h)	0.03 ± 0.0	0.81 ± 0.3	1.09 ± 0.5	0.68 ± 0.2
C_{max} (ng/mL)	16900 ± 2500	29.6 ± 5.2	40.0 ± 2.4	27.0 ± 2.9
$AUC_{0\text{-}inf}$ (ng.h/mL)	5190 ± 590	117 ± 42	149 ± 29	213 ± 14
T ½ (h)	Alpha = 0.09 ± 0.01 Beta = 4.31 ± 0.6	2.14 ± 0.6	2.60 ± 0.8	5.63 ± 1.5
F_{REL} (%)	-	-	127 ± 0.7	182 ± 0.3
F_{ABS} (%)	-	2.25 ± 0.7	2.87 ± 0.5	4.10 ± 0.2

Comparisons between oral administration of pure cromoglycate and the two lead chitosan-cromoglycate complexes (CC_{NPs}-LMW and CC_{Aggs}-LMW) are presented in Figure 6. The oral pharmacokinetic profile of CC_{Aggs}-LMW revealed a similar trend to that of pure cromoglycate, where T_{max} was reached 1.09 ± 0.5 h after dosing, followed by a rapid decline in drug plasma concentration which led to a half-life of 2.60 ± 0.8 h. The inability for CC_{Aggs}-LMW to prolong cromoglycate absorption *in vivo* may be attributed to the significant degree of premature drug release when dispersed in gastrointestinal media (Figure 2), which was hypothesized to be due the presence of unbound drug. However, despite an equivalent half-life, CC_{Aggs}-LMW achieved a 1.35-fold and 1.27-fold enhancement in C_{max} (*i.e.* 40.0 ± 2.4 ng/mL) and $AUC_{0\text{-}inf}$ (149 ± 29 ng.h/mL), compared to the pure drug. This subsequently resulted in a F_{ABS} of 2.87 ± 0.5% and demonstrates that complexing cromoglycate with chitosan through lyophilization serves as a successful approach for enhancing drug absorption.

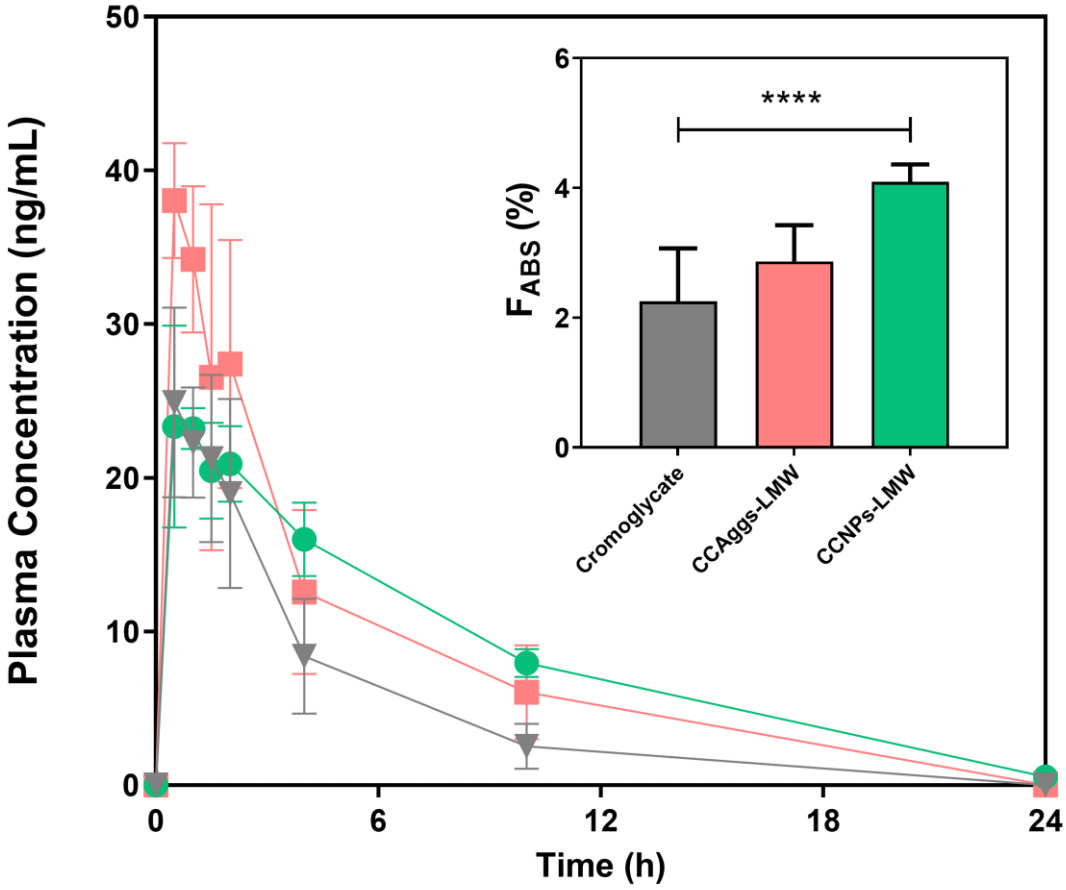


Figure 6: Plasma concentration – time profiles for pure cromoglycate (grey downwards triangles), CCAggs-LMW (red squares) and CCNPs-LMW (green circles) following a single oral dose (20 mg/kg) in Sprague Dawley rats. Data represent mean ± SD (n = 3).

Interestingly, cromoglycate complexation with chitosan nanoparticles revealed the lowest C_{max} of the orally administered formulations at 0.68 ± 0.2 h after dose. This, however, was followed by a sustained decline in the plasma cromoglycate concentration resulting in a prolonged half-life of 5.63 ± 1.5 h and an $AUC_{0\text{-}inf}$ of 213 ± 14 ng.h/mL, which ultimately corresponded to a relative bioavailability (F_{REL}) of 182 ± 0.3% compared to pure cromoglycate. The prolonged absorption of cromoglycate from CC_{NPs}-LMW resulted in a F_{ABS} of 4.10 ± 0.2% and was hypothesized to be due to the sustained drug release kinetics from CC_{NPs}-LMW (Figure 3) and enhanced capacity for chitosan nanoparticles to promote the opening of

epithelial tight junctions, as demonstrated through enhanced permeation of cromoglycate across Caco-2 monolayer (Figure 3).

Additionally, it is widely documented that chitosan particles have attractive muco-adhesive properties, due to the electrostatic attraction between chitosan and mucus lining the gastrointestinal epithelium, facilitating their adherence to and infiltration of mucus layers [9]. Gastrointestinal mucus is comprised of two layers: a thin layer with rapid turnover, and a thicker layer with static and slow movement [25]. Since CC_{Aggs}-LMW was unable to extend the half-life of cromoglycate absorption, it can be hypothesized that the smaller particle size of CC_{NPs}-LMW facilitated more efficient muco-penetration, allowing smaller nanoparticles to reach the slow-moving mucus, hence increasing the residence time at the epithelial surface and enhancing drug absorption over a longer period before being cleared. This is in agreeance with previous studies that have shown the particle size effect of chitosan muco-adhesion and penetration, where large particles are incapable of penetrating the thick gastrointestinal mucus [60].

While complexing cromoglycate with chitosan did facilitate improved oral bioavailability, this improvement was lower than anticipated when considering the *in vitro* data. These findings highlight the complexity of the gastrointestinal environment and the difficulty with replicating the dynamic processes associated with gastrointestinal transit of drug complexes *in vitro*. In particularly, the *in vitro* two-step drug release model used within this study exposed the chitosan-cromoglycate complexes to two simulated media with varying pH and surfactant compositions. However, in reality, luminal pH transitions observed *in vivo* are far more dynamic, which could trigger a reduction in the cationic charge for chitosan particles. For this application, a reduction in cationic charge has a compounding effect since the cationic charge is critical for facilitating muco-adhesion and permeation, tight junction opening and electrostatic complexation with the drug. As such, any loss of cationic charge would cause

cromoglycate to have a similar fate to the pure drug. Furthermore, the *in vitro* drug permeation model used in this study was performed in the absence of a mucus layer on top of the epithelial monolayer. Since gastrointestinal mucosa is a critical bio-barrier to particle-facilitated drug absorption, it is expected that the presence of mucus significantly impeded the degree of drug permeation.

Ultimately, this study highlights that complexing chitosan with cromoglycate serves as a promising approach for improving absolute bioavailability compared to the pure drug; yet, the improvement observed was still too low to produce therapeutically effective plasma cromoglycate concentrations and does not exceed those reported for intranasal delivery. Furthermore, the residence times of the formulations were insufficient to improve dosing strategies to a once-a-day treatment. As such, future work will be directed towards optimizing this approach by employing functionalized chitosan that has been engineered for charge stabilization and enhanced muco-penetration to reduce premature drug release and promote enhanced exposure of the drug at the absorption site.

4. Conclusions

Chitosan-cromoglycate complexes were synthesized with varying particle sizes and investigated for their potential to increase the intestinal permeation and oral absorption. Chitosan nanoparticles with a low molecular weight were most suited for creating nano-sized drug complexes capable of opening epithelial tight junctions and promoting drug transport across Caco-2 monolayers. These findings correlated with an increase in absolute cromoglycate bioavailability and prolonged absorption when orally dosed to Sprague Dawley rats. However, despite increasing oral cromoglycate absorption, the observed oral pharmacokinetics do not lend this formulation approach to serving as a once-per-day dose that obtains therapeutical plasma concentrations. Additional optimisation is therefore required to significantly improve current cromoglycate oral dosing strategies towards clinical translation.

Acknowledgments: The authors would like to thank Holman Pharmaceuticals Pty Ltd for funding this study.

5. References

[1] R. Shah, M. Mehta, D. Patel, C. Patel, Design and optimization of mucoadhesive nasal in situ gel containing sodium cromoglycate using factorial design, Asian Journal of Pharmaceutics, 5 (2011) 65-74.
[2] R. Fast, A. Gilman, J. Hardman, L. Limbird, P. Molinoff, R. Ruddon, [Goodman & Gilman's The pharmacological basis of therapeutics. 9th ed], Canadian Medical Association. Journal, 157 (1997) 1437.
[3] N. Aberg, B. Aberg, K. Alestig, The effect of inhaled and intranasal sodium cromoglyeate on symptoms of upper respiratory tract infections, Clinical <html_ent glyph="@amp;" ascii="&"/> Experimental Allergy, 26 (1996) 1045-1050.
[4] A. Abruzzo, T. Cerchiara, F. Bigucci, G. Zuccheri, C. Cavallari, B. Saladini, B. Luppi, Cromolyn-crosslinked chitosan nanoparticles for the treatment of allergic rhinitis, Eur J Pharm Sci, 131 (2019) 136-145.
[5] M. Lejeune, P.P. Lefebvre, P. Delvenne, A.E. El-Shazly, Nasal sodium cromoglycate (Lomusol) modulates the early phase reaction of mild to moderate persistent allergic rhinitis in patients mono-sensitized to house dust mite: A preliminary study, International Immunopharmacology, 26 (2015) 272-276.
[6] T.H. Yeh, L.W. Hsu, M.T. Tseng, P.L. Lee, K. Sonjae, Y.C. Ho, H.W. Sung, Mechanism and consequence of chitosan-mediated reversible epithelial tight junction opening, Biomaterials, 32 (2011) 6164-6173.
[7] A.F. Kotze, H.L. Luessen, B.J. de Leeuw, A.G. de Boer, J.C. Verhoef, H.E. Junginger, Comparison of the effect of different chitosan salts and N-trimethyl chitosan chloride on the permeability of intestinal epithelial cells (Caco-2), J Control Release, 51 (1998) 35-46.
[8] D.D. Deshmukh, W.R. Ravis, G.V. Betageri, Improved delivery of cromolyn from oral proliposomal beads, Int J Pharm, 358 (2008) 128-136.
[9] K. Sonaje, K.J. Lin, M.T. Tseng, S.P. Wey, F.Y. Su, E.Y. Chuang, C.W. Hsu, C.T. Chen, H.W. Sung, Effects of chitosan-nanoparticle-mediated tight junction opening on the oral absorption of endotoxins, Biomaterials, 32 (2011) 8712-8721.
[10] E. Lipka, J. Crison, G.L. Amidon, Transmembrane transport of peptide type compounds: prospects for oral delivery, J Control Release, 39 (1996) 121-129.
[11] A.M. Sadeghi, F.A. Dorkoosh, M.R. Avadi, M. Weinhold, A. Bayat, F. Delie, R. Gurny, B. Larijani, M. Rafiee-Tehrani, H.E. Junginger, Permeation enhancer effect of chitosan and chitosan derivatives: comparison of formulations as soluble polymers and nanoparticulate systems on insulin absorption in Caco-2 cells, Eur J Pharm Biopharm, 70 (2008) 270-278.
[12] J. Hochman, P. Artursson, Mechanisms of Absorption Enhancement and Tight Junction Regulation, Journal of Controlled Release, 29 (1994) 253-267.
[13] B. Gumbiner, Structure, biochemistry, and assembly of epithelial tight junctions, Am J Physiol, 253 (1987) C749-758.
[14] S.T. Ballard, J.H. Hunter, A.E. Taylor, Regulation of tight-junction permeability during nutrient absorption across the intestinal epithelium, in: Annual Review of Nutrition, 1995, pp. 35-55.
[15] J.L. Madara, Loosening tight junctions. Lessons from the intestine, J Clin Invest, 83 (1989) 1089-1094.
[16] V.H.L. Lee, Changing needs in drug delivery in the era of peptide and protein drugs, in: Peptide and Protein Drug Delivery, Marcel Dekker, New York, 1991, pp. 1-56.
[17] R.A. Cone, Barrier properties of mucus, Adv Drug Deliv Rev, 61 (2009) 75-85.

[18] B.C. Tang, M. Dawson, S.K. Lai, Y.Y. Wang, J.S. Suk, M. Yang, P. Zeitlin, M.P. Boyle, J. Fu, J. Hanes, Biodegradable polymer nanoparticles that rapidly penetrate the human mucus barrier, Proc Natl Acad Sci U S A, 106 (2009) 19268-19273.
[19] Y.Y. Wang, S.K. Lai, J.S. Suk, A. Pace, R. Cone, J. Hanes, Addressing the PEG mucoadhesivity paradox to engineer nanoparticles that "slip" through the human mucus barrier, Angew Chem Int Ed Engl, 47 (2008) 9726-9729.
[20] J.S. Suk, S.K. Lai, N.J. Boylan, M.R. Dawson, M.P. Boyle, J. Hanes, Rapid transport of muco-inert nanoparticles in cystic fibrosis sputum treated with N-acetyl cysteine, Nanomedicine (Lond), 6 (2011) 365-375.
[21] J.S. Suk, S.K. Lai, Y.Y. Wang, L.M. Ensign, P.L. Zeitlin, M.P. Boyle, J. Hanes, The penetration of fresh undiluted sputum expectorated by cystic fibrosis patients by non-adhesive polymer nanoparticles, Biomaterials, 30 (2009) 2591-2597.
[22] M. Yang, S.K. Lai, Y.Y. Wang, W. Zhong, C. Happe, M. Zhang, J. Fu, J. Hanes, Biodegradable nanoparticles composed entirely of safe materials that rapidly penetrate human mucus, Angew Chem Int Ed Engl, 50 (2011) 2597-2600.
[23] S.K. Lai, Y.-Y. Wang, J. Hanes, Mucus-penetrating nanoparticles for drug and gene delivery to mucosal tissues, Advanced drug delivery reviews, 61 (2009) 158-171.
[24] M. Schenk, C. Mueller, The mucosal immune system at the gastrointestinal barrier, Best Pract Res Clin Gastroenterol, 22 (2008) 391-409.
[25] L.M. Ensign, R. Cone, J. Hanes, Oral drug delivery with polymeric nanoparticles: the gastrointestinal mucus barriers, Adv Drug Deliv Rev, 64 (2012) 557-570.
[26] J. Kreuter, U. Muller, K. Munz, Quantitative and Microautoradiographic Study on Mouse Intestinal Distribution of Polycyanoacrylate Nanoparticles, International Journal of Pharmaceutics, 55 (1989) 39-45.
[27] S.A. Galindo-Rodriguez, E. Allemann, H. Fessi, E. Doelker, Polymeric nanoparticles for oral delivery of drugs and vaccines: a critical evaluation of in vivo studies, Crit Rev Ther Drug Carrier Syst, 22 (2005) 419-464.
[28] D.A. Norris, N. Puri, P.J. Sinko, The effect of physical barriers and properties on the oral absorption of particulates, Adv Drug Deliv Rev, 34 (1998) 135-154.
[29] S. Muranishi, Absorption enhancers, Crit Rev Ther Drug Carrier Syst, 7 (1990) 1-33.
[30] E.E. Hassan, J.M. Gallo, A simple rheological method for the in vitro assessment of mucin-polymer bioadhesive bond strength, Pharm Res, 7 (1990) 491-495.
[31] H.S.E. Fiebrig I., Davis S.S. , Sedimentation analysis of potential interactions between mucins and a putative bioadhesive polymer, in: L. M.D. (Ed.) Ultracentrifugation. Progress in Colloid & Polymer Science, Steinkopff, 1994.
[32] C.-M. Lehr, J.A. Bouwstra, E.H. Schacht, H.E. Junginger, In vitro evaluation of mucoadhesive properties of chitosan and some other natural polymers, International Journal of Pharmaceutics, 78 (1992) 43-48.
[33] N.G. Schipper, K.M. Varum, P. Artursson, Chitosans as absorption enhancers for poorly absorbable drugs. 1: Influence of molecular weight and degree of acetylation on drug transport across human intestinal epithelial (Caco-2) cells, Pharm Res, 13 (1996) 1686-1692.
[34] P. Artursson, T. Lindmark, S.S. Davis, L. Illum, Effect of chitosan on the permeability of monolayers of intestinal epithelial cells (Caco-2), Pharm Res, 11 (1994) 1358-1361.
[35] L. Illum, Chitosan and its use as a pharmaceutical excipient, Pharm Res, 15 (1998) 1326-1331.
[36] A.M. Dyer, M. Hinchcliffe, P. Watts, J. Castile, I. Jabbal-Gill, R. Nankervis, A. Smith, L. Illum, Nasal delivery of insulin using novel chitosan based formulations: a comparative study in two animal models between simple chitosan formulations and chitosan nanoparticles, Pharm Res, 19 (2002) 998-1008.

[37] e.a. Prasanthi, A Brief Review on Chitosan and Application in Biomedical Field, American Journal of Pharmtech Research, 6 (2016) 4.
[38] L. Illum, N.F. Farraj, S.S. Davis, Chitosan as a novel nasal delivery system for peptide drugs, Pharm Res, 11 (1994) 1186-1189.
[39] C.O.R. H.L. Lueßen, A.F. Kotze´, C.M. Lehr, A.G. de Boer, J.C. Verhoef, H.E. Junginger, Mucoadhesive polymers in peroral peptide drug delivery IV. Polycarbophil and chitosans are potent enhancers of peptide transport across intestinal mucosae in vitro, J. Control. Release, (1997) 15-23.
[40] B. Luppi, Federica Bigucci, Teresa Cerchiara, Vittorio Zecchi, Chitosan-based hydrogels for nasal drug delivery: from inserts to nanoparticles, Expert Opin Drug Deliv, 7 (2010) 811-828.
[41] F.W. Merkus, J.C. Verhoef, N.G. Schipper, E. Marttin, Nasal mucociliary clearance as a factor in nasal drug delivery, Adv Drug Deliv Rev, 29 (1998) 13-38.
[42] K. Sonaje, Y.J. Chen, H.L. Chen, S.P. Wey, J.H. Juang, H.N. Nguyen, C.W. Hsu, K.J. Lin, H.W. Sung, Enteric-coated capsules filled with freeze-dried chitosan/poly(γ-glutamic acid) nanoparticles for oral insulin delivery, Biomaterials, 31 (2010) 3384-3394.
[43] K. Sonaje, K.J. Lin, S.P. Wey, C.K. Lin, T.H. Yeh, H.N. Nguyen, C.W. Hsu, T.C. Yen, J.H. Juang, H.W. Sung, Biodistribution, pharmacodynamics and pharmacokinetics of insulin analogues in a rat model: Oral delivery using pH-Responsive nanoparticles vs. subcutaneous injection, Biomaterials, 31 (2010) 6849-6858.
[44] S.F. Peng, M.T. Tseng, Y.C. Ho, M.C. Wei, Z.X. Liao, H.W. Sung, Mechanisms of cellular uptake and intracellular trafficking with chitosan/DNA/poly(γ-glutamic acid) complexes as a gene delivery vector, Biomaterials, 32 (2011) 239-248.
[45] M.C. Chen, H.S. Wong, K.J. Lin, H.L. Chen, S.P. Wey, K. Sonaje, Y.H. Lin, C.Y. Chu, H.W. Sung, The characteristics, biodistribution and bioavailability of a chitosan-based nanoparticulate system for the oral delivery of heparin, Biomaterials, 30 (2009) 6629-6637.
[46] J. Smith, E. Wood, M. Dornish, Effect of chitosan on epithelial cell tight junctions, Pharm Res, 21 (2004) 43-49.
[47] K. Sonaje, Y.H. Lin, J.H. Juang, S.P. Wey, C.T. Chen, H.W. Sung, In vivo evaluation of safety and efficacy of self-assembled nanoparticles for oral insulin delivery, Biomaterials, 30 (2009) 2329-2339.
[48] L. Wright, P. Joyce, T.J. Barnes, R. Lundmark, C.A.S. Bergström, M. Hubert, C.A. Prestidge, A Comparison of Chitosan, Mesoporous Silica and Poly(lactic-co-glycolic) Acid Nanocarriers for Optimising Intestinal Uptake of Oral Protein Therapeutics, Journal of Pharmaceutical Sciences, 110 (2021) 217-227.
[49] R. Fernandez-Urrusuno, P. Calvo, C. Remunan-Lopez, J.L. Vila-Jato, M.J. Alonso, Enhancement of nasal absorption of insulin using chitosan nanoparticles, Pharm Res, 16 (1999) 1576-1581.
[50] J. Fallingborg, Intraluminal pH of the human gastrointestinal tract, Danish medical bulletin, 46 (1999) 183-196.
[51] I.J. Hidalgo, T.J. Raub, R.T. Borchardt, Characterization of the human colon carcinoma cell line (Caco-2) as a model system for intestinal epithelial permeability, Gastroenterology, 96 (1989) 736-749.
[52] M. Rousset, The human colon carcinoma cell lines HT-29 and Caco-2: two in vitro models for the study of intestinal differentiation, Biochimie, 68 (1986) 1035-1040.
[53] A. Quaroni, Crypt cell antigen expression in human colon tumor cell lines: analysis with a panel of monoclonal antibodies to CaCo-2 luminal membrane components, J Natl Cancer Inst, 76 (1986) 571-585.
[54] A. Quaroni, M.M. Weiser, S. Lee, D. Amodeo, Expression of developmentally regulated crypt cell antigens in human and rat intestinal tumors, J Natl Cancer Inst, 77 (1986) 405-415.

[55] N.G. Schipper, K.M. Vårum, P. Artursson, Chitosans as absorption enhancers for poorly absorbable drugs. 1: Influence of molecular weight and degree of acetylation on drug transport across human intestinal epithelial (Caco-2) cells, Pharmaceutical research, 13 (1996) 1686-1692.
[56] S.Y. Chae, M.-K. Jang, J.-W. Nah, Influence of molecular weight on oral absorption of water soluble chitosans, Journal of controlled release, 102 (2005) 383-394.
[57] D. Mei, S. Mao, W. Sun, Y. Wang, T. Kissel, Effect of chitosan structure properties and molecular weight on the intranasal absorption of tetramethylpyrazine phosphate in rats, European journal of pharmaceutics and biopharmaceutics, 70 (2008) 874-881.
[58] M. Huang, E. Khor, L.-Y. Lim, Uptake and cytotoxicity of chitosan molecules and nanoparticles: effects of molecular weight and degree of deacetylation, Pharmaceutical research, 21 (2004) 344-353.
[59] T.-H. Yeh, L.-W. Hsu, M.T. Tseng, P.-L. Lee, K. Sonjae, Y.-C. Ho, H.-W. Sung, Mechanism and consequence of chitosan-mediated reversible epithelial tight junction opening, Biomaterials, 32 (2011) 6164-6173.
[60] M.A. Mohammed, J.T.M. Syeda, K.M. Wasan, E.K. Wasan, An Overview of Chitosan Nanoparticles and Its Application in Non-Parenteral Drug Delivery, Pharmaceutics, 9 (2017) 53.